Scripta Materialia 145 (2018) 99–103

Contents lists available at ScienceDirect

Scripta Materialia

journal homepage: www.elsevier.com/locate/scriptamat

Regular article

Abnormal grain coarsening in cyclically deformed gradient nanograined Cu

J.Z. Long [a,b], Q.S. Pan [a], N.R. Tao [a], L. Lu [a,*]

[a] Shenyang National Laboratory for Materials Science, Institute of Metal Research, Chinese Academy of Sciences, Shenyang 110016, PR China
[b] University of Chinese Academy of Sciences, 19A Yuquan Road, Shijingshan District, Beijing 100049, PR China

ARTICLE INFO

Article history:
Received 4 August 2017
Received in revised form 6 October 2017
Accepted 14 October 2017
Available online xxxx

Keywords:
Gradient nanograin (GNG)
Cu
Cyclic deformation
Abnormal grain coarsening
Extrusions/intrusions

ABSTRACT

Microstructural evolution of gradient nanograined (GNG) Cu was investigated under strain-controlled cyclic deformation. Mechanically driven abnormal grain coarsening initiated from the ultrafine grained subsurface layer and eventually extended to the nanograined top surface with increasing cycles. Abnormal grain coarsening and the formation of dislocation patterns sustain the cyclic plastic strain and postpone the formation of extrusions/intrusions at the top surface, contributing to the enhancement of overall cyclic properties of GNG Cu.

Homogenously refining grain sizes into the ultrafine and nanometer scale can make materials several times stronger in strength [1,2]. But this comes at a dramatic loss of ductility, due to diminished work-hardening capability and strain localization [3]. In particular, under low-amplitude stress/strain cyclic deformation, severe strain localization occurs in various ultrafine grained (UFG) and nanograined (NG) metals/alloys in the form of macroscopically shear banding and abnormal grain coarsening [4–9]. Fatigue cracks preferentially initiate along those shear bands/abnormal grains at the surface and lead to the final failure. Such localized deformation modes greatly influence the fatigue damage resistance of high-strength nanostructured metals [10–12].

Recent studies showed that compared with homogeneous counterparts, gradient nanograined (GNG) metals, with grain size spatially increasing from nanoscale in surface to CG in core, exhibit superior mechanical properties, such as high strength and considerable ductility [13–15]. A uniform tensile plasticity (~30%) comparable to the CG core has been achieved for the surface nanograins in the uniaxial tensile test of GNG Cu, where the strain localization was effectively suppressed [15]. Homogeneous grain coarsening in GNG Cu was responsible for such large tensile plasticity, which is reasonably interpreted as a mechanically driven grain boundary (GB) migration process [15–17].

Due to the presence of high strength GNG layer, the high-cycle fatigue properties of GNG metals/alloys under cyclic loading tests were also enhanced, compared to their CG counterparts [18,19]. For instance, the fatigue limit of GNG Cu at 10^7 cycles reaches up to 98 MPa, even slightly higher than that of the UFG counterparts [18]. An abnormal grain coarsening phenomenon was found in the subsurface UFG layer of GNG Cu after fatigue to failure [18], rather than homogeneous grain coarsening under uniaxial tensile testing [15]. It suggests that the cyclic deformation induces abnormal grain coarsening that initiated from the subsurface layer and grew toward the top surface layer [18]. Up to now, the study of microstructural evolution of gradient NGs and UFGs during cyclic loading before failure and the underlying failure mechanism of the GNG metals are still in their infancy. In this study, systematic strain-controlled cyclic deformations were performed on GNG Cu to different cyclic lives. The corresponding microstructure development and the cyclic deformation mechanism of GNG Cu samples were analyzed.

Commercial purity CG Cu rods (99.97 wt%) with an average grain size of 21 μm after annealing at 723 K for 1 h were machined into dog-bone shape samples with a gauge diameter of 6 mm and a gauge length of 12 mm. Then, both the gauge sections and arc transitions were subjected to surface mechanical gridding treatment (SMGT) process at cryogenic temperature for preparing gradient nanograined sample, which was described in detail in [15,18].

Total strain controlled symmetric tension-compression fatigue tests of GNG Cu were performed on an Instron 8874 testing machine at ambient temperature. A dynamic strain gauge extensometer with a gauge length of 10 mm was applied to measure and control the cyclic strain amplitude. A triangular wave with a frequency of 2 Hz was used. The imposed total strain amplitude ($\Delta\varepsilon_t/2$) was set as 0.12%, which was approximately comparable to the calculated $\Delta\varepsilon_t/2$ value of GNG Cu at the

* Corresponding author.
E-mail address: llu@imr.ac.cn (L. Lu).

https://doi.org/10.1016/j.scriptamat.2017.10.019
1359-6462/

imposed stress amplitude of 140 MPa in [18] according to the Hooke's law. First of all, one set of GNG Cu samples were cycled to failure at $\Delta\varepsilon_t/2 = 0.12\%$, which exhibits a fatigue-to-failure lifetime (N_f) of ~1×10^6 cycles. Besides, the other GNG samples were cyclically deformed at the same strain amplitude, but interrupted at the planned cycles of loading (i.e. $N = 4\%N_f$, $N = 20\%N_f$, $N = 40\%N_f$) and then fully unloaded, respectively.

The cross-section microstructures of GNG Cu with different cycles were characterized by using the FEI Nova NanoSEM 430 scanning electron microscope (SEM) and FEI Tecnai F20 transmission electron microscope (TEM), respectively. Note that the applied aperture diameter for obtaining SAED patterns in TEM is 5 μm. 3-dimensional surface features on cyclic deformed GNG Cu were investigated by using Olympus LEXT OLS4100 confocal laser scanning microscope (CLSM). Textures of GNG Cu before and after cyclic deformation were analyzed by electron backscatter diffraction (EBSD) under a voltage of 20 kV and a current of 6.0 nA with a step size of 20 nm, respectively.

SMGT processing produced a spatially gradient microstructure along the radical direction of GNG Cu rod sample, which is composed of a NG layer (with a depth of 20 μm in top surface layer), a UFG layer (at depth from 20 to 220 μm), a deformed CG layer and an undeformed CG core (Fig. 1a). For convenience, both NG and UFG layers with a total thickness of 220 μm gradient nanograined layer are hereafter referred to as the GNG layer. As shown in Figs. 2a and 3a, the GBs of ultrafine- and nano-grains in the GNG layer are curved with a very high density of dislocations, which are apparently in the non-equilibrium state, similar to those observed in nanostructured metals prepared by means of severe plastic deformation [6]. The selected area electron diffraction (SAED) patterns (inset in Figs. 2a and 3a) and EBSD result (Fig. 3e) revealed that these grains are randomly oriented. The pole figures of GNG layer in the as-SMGT GNG Cu are mainly from the subsurface UFG layer, due to the fact that most of NGs in the top NG layer are too small to be measured using the traditional EBSD techniques.

The cross-sectional microstructure evolutions of GNG Cu with different cycles were systematically investigated by SEM observations, as shown in Fig. 1. The microstructure of the GNG layer at $4\%N_f$ cycles (Fig. 1b) was nearly same with that in the as-SMGT state (Fig. 1a), suggesting that no detectable microstructural change occurs in the GNG layer. However, after $20\%N_f$ cycles, some obvious abnormal large grains began to appear locally in the subsurface UFG layer within a depth of ~33 to ~75 μm (Fig. 1c), which is approximately consistent with the depth of abnormal grain coarsening in fatigued GNG Cu under stress control [18]. On further increasing cycles, these grains became coarser and coarser. Specially, coarse grains mainly extended simultaneously toward the top surface and deeper interior along the maximum shear stress direction approximately, i.e. at ~45° relative to the loading axis (Fig. 1d). At $100\%N_f$, some abnormal coarsened grains have reached the topmost surface, with a larger grain size of 18.6 ± 9.0 μm (Fig. 1e).

In order to track the detailed microstructural evolution of GNG layer during cyclic deformation, closer TEM observations were performed on UFG layer and NG layer (as indicated by the squares in Fig. 1a) at different cycles, as shown in Figs. 2 and 3, respectively. After $20\%N_f$ cycles, abnormally coarsened grains with a low density of dislocation tangles/veins were widespreadly detected in the subsurface UFG layer (Fig. 2b). With increasing cycles, i.e. at $100\%N_f$, the grain growth continuously occurred, consuming the surrounding UFG. Meanwhile well-developed dislocation patterns such as walls are formed inside the coarse grains (Fig. 2c), similar with that observed in cyclically deformed CG counterparts [20]. In contrast, the statistic grain size of remnant ultrafine grains in the vicinity of microsized grains, as shown in Fig. 2d, is almost comparable to that in the as-SMGT state (Fig. 2a), suggesting that they are relatively stable during cyclic deformation. Interestingly, some clear and straight twin boundaries can be found in some large grains, as confirmed by the SAED patterns (inset in Fig. 2b).

However, the nano-grains in the NG layer in Fig. 3b are still roughly equiaxed with a high density of dislocations and separated by curved GBs at $20\%N_f$, bearing a strong resemblance with that in the as-SMGT state (Fig. 3a). Until at 100% N_f, only a few abnormally coarse grains were detected there, in which dislocation substructures were universally observed (Fig. 3c). In contrast, the residual nano-grain matrix adjacent to the abnormal coarsening grains still exhibits similar grain morphology and grain size (40 ± 10 nm) to that in the as-SMGT state (Fig. 3d). EBSD measurements showed that different from the randomly oriented NG and UFG matrix, abnormal coarsened grains after cyclic deformation have a highly preferential orientation, approximately a cube (001)[100] texture (Fig. 3e). Schmid factor analysis revealed that most of these micron-sized grains have a relative soft orientation with a large Schmid factor ranging from 0.33 to 0.49.

This unusual abnormal grain coarsening fatigue mechanism of GNG Cu is distinct from that in homogeneous UFG (or NG) metals [6,21] and bimodal structure with coarse grains randomly embedded in UFG or NG matrix [22]. Macroscopic shear banding and abnormal grain coarsening randomly appeared on sample surface or inside the homogeneous UFG and NG structures [5,23]. While for the metals with a bimodal structure, cyclic plastic strain mainly concentrates in coarse grains on the sample surface or inside materials, due to its lower yield stress, relative to

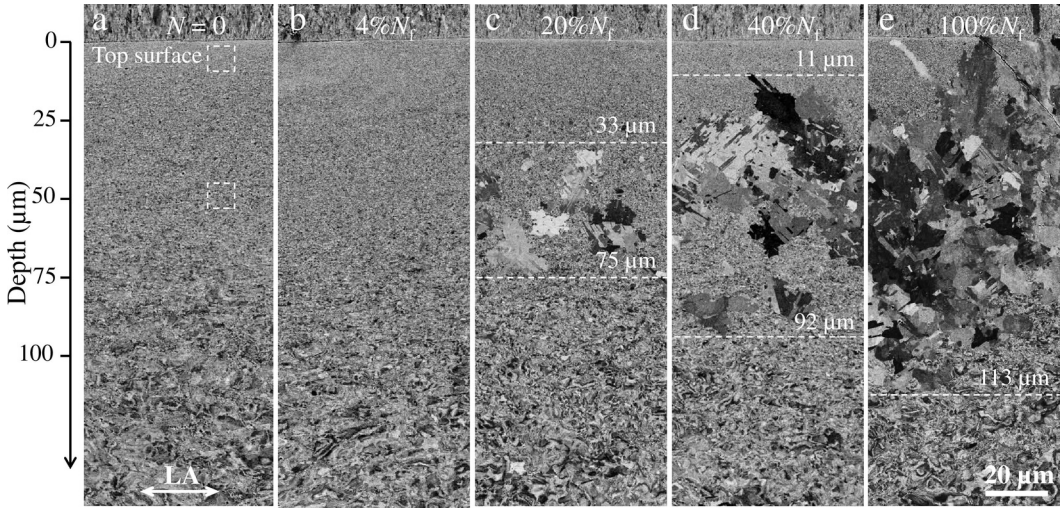

Fig. 1. Typical SEM images of microstructure evolution of GNG Cu cyclically deformed at $\Delta\varepsilon_t/2 = 0.12\%$ with a fatigue number (N) of (a) 0 cycle, (b) $4\%N_f$, (c) $20\%N_f$, (d) $40\%N_f$ and (e) $100\%N_f$. The inserted dashed lines in c-e indicate the regions with abnormal grain coarsening. The NG and UFG structures in dashed square inserted in (a) and their evolution under cyclic loading will be investigated via TEM, respectively. LA is cyclic loading axis.

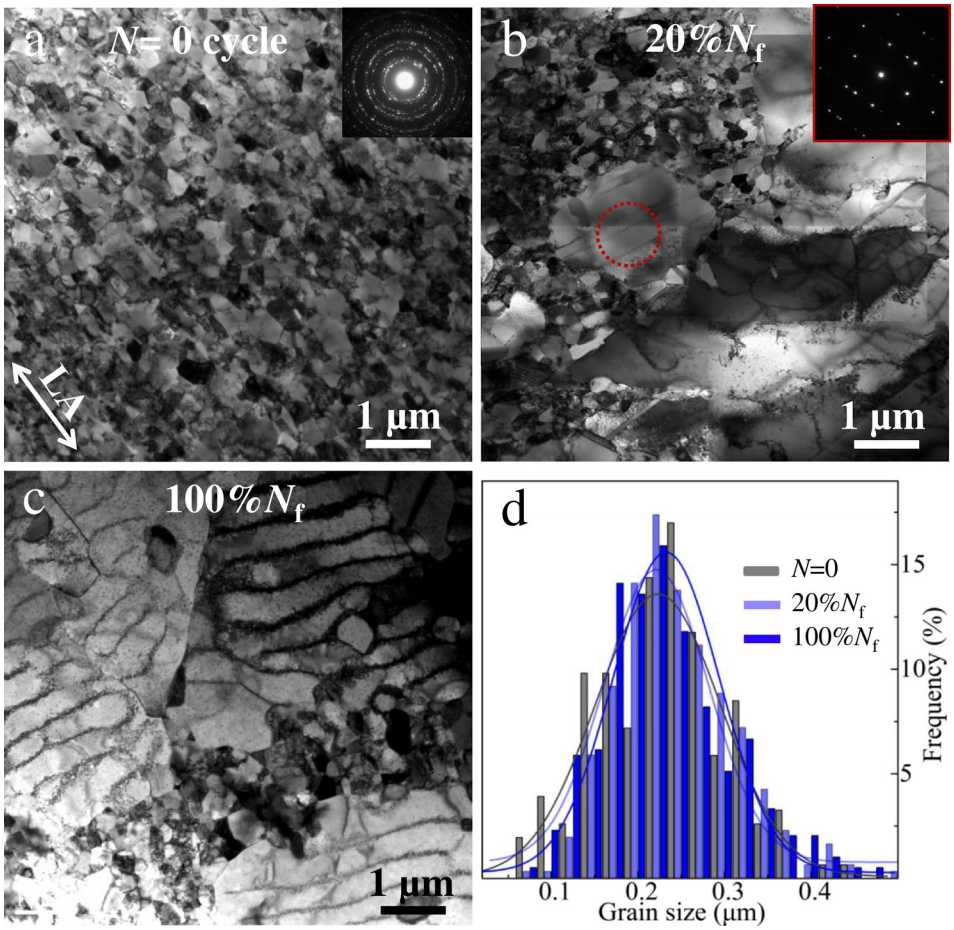

Fig. 2. TEM images of subsurface UFG layer at a depth of 50 μm with different cycles (a) 0 cycle, (b) 20%N_f and (c) 100%N_f. Inserts in (a-b) are SAED patterns. (d) corresponding size distributions of ultrafine grains at different cycles.

surrounding UFG/NG matrix [22]. Such strain localization easily results in early fatigue crack initiation at the CG on the sample surface and almost no increase in fatigue limit, relative to the CG counterpart.

Comparing with the monotonic tensile tests, the most significant features of the cyclic tests are the smaller cyclic stress/strain amplitude (only 0.12% in this study) but large accumulative plastic strain ($\sum 4\Delta\varepsilon_{pl}/2$, where $\Delta\varepsilon_{pl}/2$ is the cyclic plastic strain amplitude) [20]. $\sum 4\Delta\varepsilon_{pl}/2$ of GNG Cu fatigued to failure, roughly estimated from the data of hysteresis loop and total cycles, was as large as about 1000, which may be three orders of magnitude higher than the plastic strain in tensile tests (several tens percent) [15]. Since the yield strength of the NG layer with smaller grain size is generally higher than that of UFG layer, the plastic deformation of UFG layer may occur prior to that of NG layer, according to Hall-Petch relationship [2]. That means when the imposed strain/stress is small enough, UFG layer deforms plastically firstly and NG layer deforms elastically, just as the case in this study. The accumulative plastic strain mainly concentrates on UFG layer firstly and then transmits to the neighboring layers during cyclic deformation. Thus, both GNG layer itself and specialties of cyclic loading tests lead to the occurrence of abnormal grain coarsening in UFG subsurface layer under cyclic loading.

The abnormal grain coarsening of GNG Cu during cyclic deformation may also be interpreted as a mechanically driven GB migration process, as reported in NG metals under experimental tensile tests [15,16] and fatigue test in molecular dynamic simulations [24]. This is closely related to the orientation and non-equilibrium grain boundaries of the UFGs after the SMGT process. A strong cube (001)[100] texture with larger Schmid factor has been detected for abnormal coarsened grains in fatigued GNG layer, as shown in Fig. 3e, which suggested that the cyclic-driven GB migration process might preferentially occur in the grains with soft orientations. Besides that, decreasing the energy of the highly non-equilibrium GBs, via reduction of the defects density [18] and the emission of Shockley partials from GBs [24,25], also benefits to GB migration and causes grain coarsening. As a result, grain coarsening would extend toward high-energy NG top surface along the direction of maximum shear stress to decrease the whole stored energy in sample.

The surface features characterized by CLSM and SEM show that the average surface roughness (*Ra*) of GNG sample after fatigue is still comparable to that in the as-SMGT state, only 0.3 μm. Randomly distributed extrusions/intrusions were observed at the surface of GNG Cu after fatigue to failure (Fig. 4a & b). Their fluctuation, defined as the altitude difference between the adjacent surface peaks and valleys, ranges from 0.1 to 1.5 μm (Fig. 4a and c), which is comparable to the typical micron-scale extrusions/intrusions in fatigued CG metals [20]. Fig. 4d clearly shows that these extrusions/intrusions, accompanied by the fatigue crack nucleation, are formed in the coarse grains when they extend to the top surface, more like that occurs in CG fcc metals [20] and obviously distinct from the shear bands in fatigued nanostructured metals [4–8,10,26]. Shear bands usually occurred shortly after cyclic loading, either in long, loose strips or in short, dense form and mainly distributed at ~45° relative to the stress axis [4–7,10]. No detectable grain coarsening was observed in the vicinity of shear bands [26]. Although the abnormal coarsened grains in GNG Cu sample are indeed reminiscent of that in fatigued nanostructured metals [9], but a much larger grain size (18.6 ± 9.0 μm) was seen in GNG Cu. These evidences strongly suggest that the extrusions/intrusions fatigue feature of GNG Cu is induced by dislocation slips in abnormal coarse grains at the topmost surface, rather than the shear bands.

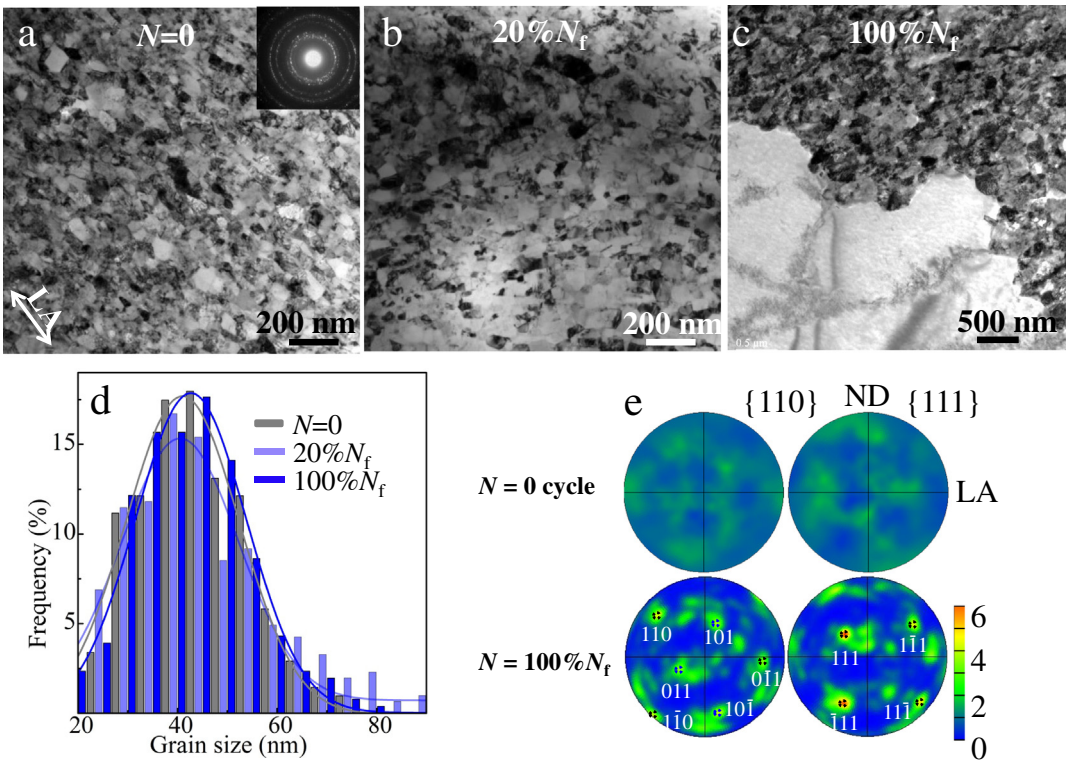

Fig. 3. TEM images of surface NG layer at a depth of 3–5 μm with different cycles (a) 0 cycle, (b) 20%N_f and (c) 100%N_f. (d) corresponding size distributions of nanograins at different cycles; (e) Pole figures of GNG layer (mainly the subsurface UFG layer) at $N = 0$ (upper ones) and $N = 100\%N_f$ (lower ones). ND points to the top surface.

It is known that the most fatigue failures or structure instability occur on the surface of material and then propagate into the interior [20]. Here in this study, we have to emphasize when the grain coarsening (structure instability) initiates from the subsurface layer and sustains the plastic strain during the cyclic loading, the top surface layer with high strength NG grains is still under elastic deformation and

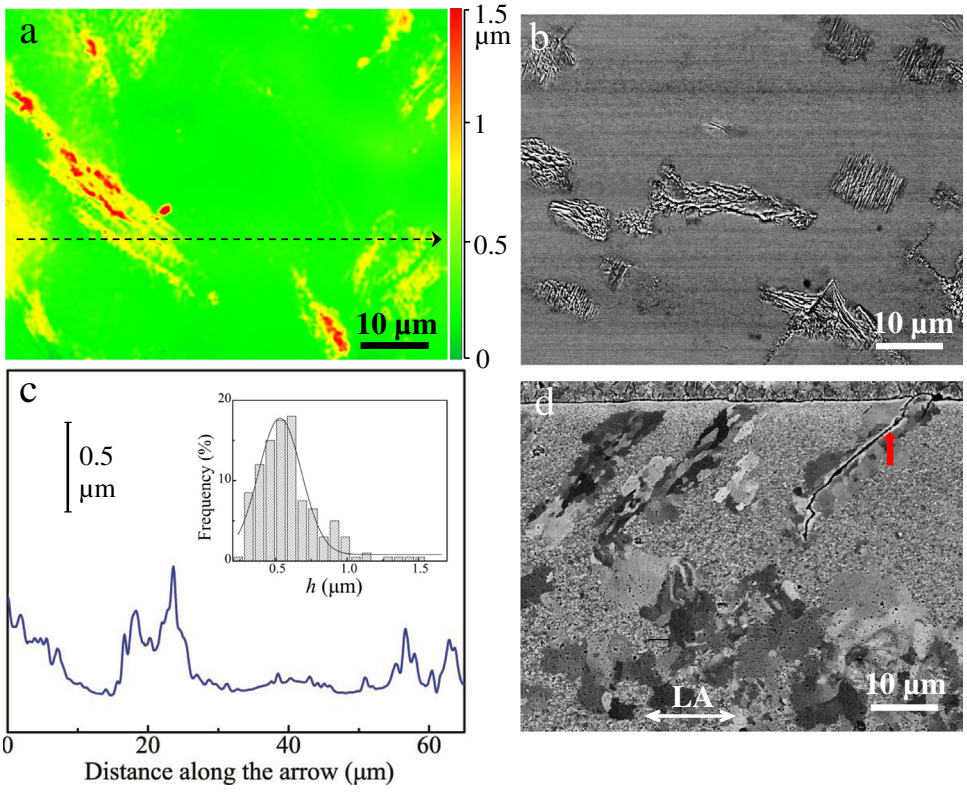

Fig. 4. Surface features and cracking of GNG Cu after fatigue. (a) Top view CLSM and (b) SEM images, (c) "Hill" and "valley" profile along the arrow in (a), (d) Cross-sectional SEM image of gradient nanograined layer after fatigue, showing fatigue crack initiation in abnormal coarsening grains.

without any surface strain localization. From the experimental observations in Fig. 1d, it can be found that even after 40% N_f, namely after ~4×10^5 cycles with an accumulative plastic strain as large as ~400, the abnormal grain coarsening has not reached the topmost NG surface (~10 μm away), which have offered a time as long as ~3330 min and more space for the beginning of the surface instability. Besides, compared with the soft CG core, the remnant stable UFGs and NGs surface layer undergoing elastic deformation can effectively suppress the surface crack initiation, which benefits for the whole sample undertaking a high cyclic stress and an improving fatigue lifetime. Thus, it is understandable that why a much higher fatigue limit is achieved in GNG Cu, albeit exhibiting a tensile strength comparable with that of CG counterpart [18].

Both the abnormal grain coarsening and the formation of dislocation patterns inside coarse grains jointly sustain the cumulative cyclic plastic strain. Thus, the abnormal coarsened grains with a much larger size are achieved during fatigue, mainly owing to very large localized accumulative plastic strain (~1000), compared to the case in the tensile test [15]. However, the essential mechanism of the mechanically driven abnormal grain coarsening in GNG Cu during cyclic deformation is still far from mature and worthy of in-depth study.

In summary, detailed microstructural evolution analysis of GNG Cu under strain controlled cyclic deformation revealed that both the abnormal grain coarsening and the formation of dislocation patterns inside coarse grains jointly sustain the cumulative cyclic plastic strain. The presence of spatial GNG structure effectively postpones fatigue crack initiation in top surface and greatly enhances the fatigue limits, shedding lights on a new method for designing engineering materials with superior fatigue properties.

Acknowledgements

L.L. acknowledges the financial support by the National Science Foundation of China (Grant Nos. 51371171, 51471172, 51420105001 and U1608257) and the key Research program of Frontier Science, CAS. The authors are grateful to Mr. X. Si for assistance in sample preparation.

References

[1] H. Gleiter, Prog. Mater. Sci. 33 (1989) 223–315.
[2] M.A. Meyers, A. Mishra, D.J. Benson, Prog. Mater. Sci. 51 (2006) 427–556.
[3] A. Pineau, A. Amine Benzerga, T. Pardoen, Acta Mater. 107 (2016) 508–544.
[4] S.R. Agnew, A.Y. Vinogradov, S. Hashimoto, J.R. Weertman, J. Electron. Mater. 28 (1999) 1038–1044.
[5] A. Vinogradov, S. Hashimoto, Mater. Trans. JIM 42 (2001) 74–84.
[6] H. Mughrabi, H.W. Höppel, Int. J. Fatigue 32 (2010) 1413–1427.
[7] L. Kunz, P. Lukáš, M. Svoboda, Mater. Sci. Eng. A 424 (2006) 97–104.
[8] C.C.F. Kwan, Z. Wang, Philos. Mag. 93 (2012) 1065–1079.
[9] B.L. Boyce, H.A. Padilla, Metall. Mater. Trans. A. 42A (2011) 1793–1804.
[10] M. Goto, N. Teshima, S.Z. Han, K. Euh, T. Yakushiji, S.S. Kim, J. Lee, Eng. Fract. Mech. 110 (2013) 218–232.
[11] T. Hanlon, Y.N. Kwon, S. Suresh, Scr. Mater. 49 (2003) 675–680.
[12] H. Mughrabi, H.W. Höppel, M. Kautz, Scr. Mater. 51 (2004) 807–812.
[13] Y. Wei, Y. Li, L. Zhu, Y. Liu, X. Lei, G. Wang, Y. Wu, Z. Mi, J. Liu, H. Wang, H. Gao, Nat. Commun. 5 (2014).
[14] X.L. Wu, P. Jiang, L. Chen, F.P. Yuan, Y.T.T. Zhu, Proc. Natl. Acad. Sci. U. S. A. 111 (2014) 7197–7201.
[15] T.H. Fang, W.L. Li, N.R. Tao, K. Lu, Science 331 (2011) 1587–1590.
[16] T.J. Rupert, D.S. Gianola, Y. Gan, K.J. Hemker, Science 326 (2009) 1686–1690.
[17] W. Chen, Z.S. You, N.R. Tao, Z.H. Jin, L. Lu, Acta Mater. 125 (2017) 255–264.
[18] L. Yang, N.R. Tao, K. Lu, L. Lu, Scr. Mater. 68 (2013) 801–804.
[19] T. Roland, D. Retraint, K. Lu, J. Lu, Scr. Mater. 54 (2006) 1949–1954.
[20] S. Suresh, Fatigue of Materials, second ed Cambridge University Press, Cambridge, 1998.
[21] S. Kobayashi, A. Kamata, T. Watanabe, Acta Mater. 91 (2015) 70–82.
[22] M. Korn, R. Lapovok, A. Bohner, H.W. Höppel, H. Mughrabi, Kovove Mater. 49 (2011) 51–63.
[23] T.A. Furnish, A. Mehta, D. Van Campen, D.C. Bufford, K. Hattar, B.L. Boyce, J. Mater. Sci. 52 (2017) 46–59.
[24] J. Schiøtz, Mater. Sci. Eng. A 375 (2004) 975–979.
[25] X.H. An, Q.Y. Lin, S.D. Wu, Z.F. Zhang, Scr. Mater. 68 (2013) 988–991.
[26] S.D. Wu, Z.G. Wang, C.B. Jiang, G.Y. Li, I.V. Alexandrov, R.Z. Valiev, Scr. Mater. 48 (2003) 1605–1609.